NJC

COMMUNICATION

View Article Online
View Journal | View Issue

Cite this: *New J. Chem.*, 2023, **47**, 9555

Received 20th March 2023,
Accepted 2nd May 2023

DOI: 10.1039/d3nj01299a

rsc.li/njc

Synthesis of 1,1′-diaryl-4,4′-bibenzo[*c*]thiophene derivatives with aryl substituents on the thiophene rings by Stille or Suzuki coupling reaction†

Taiki Higashino,[a] Yasuto Hara,[a] Keiichi Imato,[a] Seiji Akiyama,[b] Mio Ishida[b] and Yousuke Ooyama *[a]

Benzo[*c*]thiophene and its derivatives are attractive chromophores or π-building blocks for emitters, photosensitizers, and semiconductors used in organic optoelectronic devices. Herein, we provide facile synthetic methods of 1,1′-diaryl-4,4′-bibenzo[*c*]thiophene derivatives by Stille or Suzuki coupling reaction and their photophysical properties in the solution and the solid state, electrochemical properties, and X-ray crystal structures.

Benzo[*c*]thiophene and its derivatives have attracted not only growing scientific interest in synthetic organic chemistry, polymer chemistry, electrochemistry, photochemistry, and theoretical chemistry,[1] but also considerable attention as a promising chromophore or π-building block of emitters, photosensitizers, and semiconductors for organic optoelectronic devices, including organic light-emitting diodes (OLEDs),[2] organic photovoltaics (OPVs),[3] dye-sensitized solar cells (DSSCs),[4] and organic field-effect transistors (OFETs).[5] Accordingly, some benzo[*c*]thiophene derivatives with substituents on the thiophene ring and/or the benzene ring such as 1,3- or 5,6-disubstituted benzo[*c*]thiophenes[6] and 1,3,4,7- or 1,3,5,6-tetrasubstituted benzo[*c*]thiophenes[7] have been synthesized (Fig. 1a). Moreover, a few 3,3′-disubstituted-1,1′-bibenzo[*c*]thiophenes as the 1,1′-dimer of bibenzo[*c*]thiophene (abbr. as BBT) have been developed by Cava,[8] Ono,[4,9] and Mohanakrishnan *et al.*,[10] and they offered their synthetic methods and photophysical and electrochemical properties. On the other hand, in our previous work,[11a,b] we have developed 1,1′-disubstituted 4,4′-BBT derivatives (**BBT-Si**, **BBT-Sn**, and **BBT-CHO**) with various substituents (R = $Si(CH_3)_2C(CH_3)_3$, $Sn(CH_3)_3$, and CHO, Fig. 1a) as well as unsubstituted 4,4′-BBT (**BBT-H**) by a straightforward reaction method from 1,1′,3,3′-tetrahydro-[4,4′-bibenzo[*c*]thiophene] 2,2′-dioxide (**SO-BBT-H4**, Scheme 1), and revealed their photophysical and electrochemical properties. Furthermore, we achieved the development of 1,1′-diaryl-4,4′-BBT by Stille coupling reaction of 1,1′-distannyl-4,4′-BBT (**BBT-Sn**) with aryl halide (Method A in Scheme 1).[11c] For example, the Stille coupling reaction of **BBT-Sn** with 1-bromo-4-*tert*-butylbenzene gave **BBT-Ph^{t}Bu** in a moderate yield (Fig. 1b). Indeed, the expansion of the π-conjugated system by the introduction of aryl substituents on chromophores is an effective way to adjust the highest occupied molecular orbital (HOMO) and lowest unoccupied molecular orbital (LUMO) energy levels, that is, the photophysical and electrochemical properties for the development of high-performance optoelectronic devices. However, 1,1′-diaryl-4,4′-BBT could be obtained only by Stille coupling reaction using **BBT-Sn** so far. Therefore, for this purpose it is necessary to develop facile synthetic methods for 1,1′-diaryl-4,4′-BBT derivatives.

In this work, with the aim of providing a new synthetic method of 1,1′-diaryl-4,4′-BBT derivatives and their photophysical and

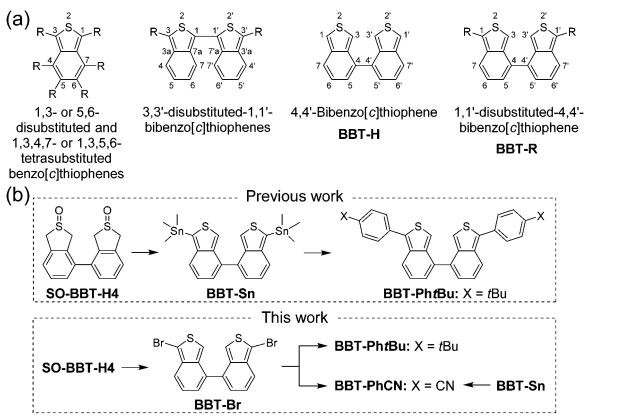

Fig. 1 (a) Chemical structures of benzo[c]thiophenes, 1,1′-bibenzo[c]thiophenes, and 4, 4′-bibenzo[c]thiophenes. (b) Previous work (ref. 11c) and this work for the synthesis of 1,1′-diaryl-4,4′-BBT.

[a] *Applied Chemistry Program, Graduate School of Advanced Science and Engineering, Hiroshima University, 1-4-1 Kagamiyama, Higashi-Hiroshima 739-8527, Japan. E-mail: yooyama@hiroshima-u.ac.jp*
[b] *Science & Innovation Center, Mitsubishi Chemical Corporation, 1000 Kamoshida-cho, Aoba-ku, Yokohama-shi, Kanagawa 227-8502, Japan*

† Electronic supplementary information (ESI) available. CCDC 2248179. For ESI and crystallographic data in CIF or other electronic format see DOI: https://doi.org/10.1039/d3nj01299a

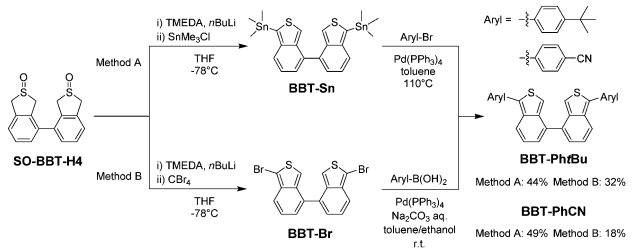

Scheme 1 Synthetic routes to 1,1′-diaryl-4,4′-bibenzo[*c*]thiophene derivatives **BBT-Ph^{t}Bu** and **BBT-PhCN** by Stille coupling reaction (Method A) and Suzuki coupling reaction (Method B).

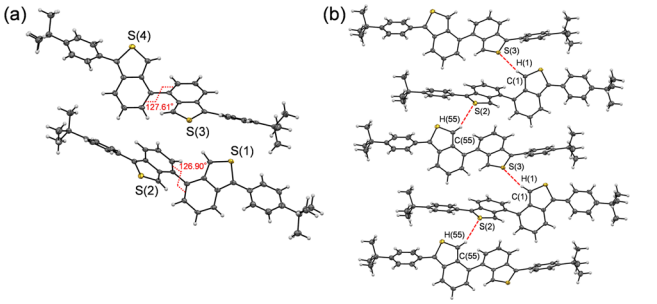

Fig. 2 Crystal structure of **BBT-Ph^{t}Bu**: (a) molecular structure and (b) intermolecular interactions.

electrochemical properties, we successfully synthesized 1,1′-dibromo-4,4′-BBT (**BBT-Br**) as an intermediate in the synthesis of the BBT derivative form **SO-BBT-H4** (Fig. 1b); **BBT-Br** as a synthetic building block enables us to develop various BBT series for optoelectronic materials by a variety of synthetic approaches, including homo- and cross-coupling reactions, nucleophilic aromatic substitution, and organometallic reagent formation. Indeed, we have achieved the synthesis of **BBT-PhCN** with an electron-withdrawing cyanophenyl group using **BBT-Br** and evaluation of its photophysical and electrochemical properties, as well as **BBT-Ph^{t}Bu** with an electron-donating *tert*-butylphenyl group. Herein, we provide facile methods of 1,1′-diaryl-4,4′-BBT derivatives by Stille coupling reaction of **BBT-Sn** with aryl halide and Suzuki coupling reaction of **BBT-Br** with arylboronic acid and their photophysical properties in the solution and the solid state, electrochemical properties and X-ray crystal structures.

As previously indicated, we have demonstrated that **BBT-Sn** is a useful intermediate in the synthesis of 1,1′-diaryl-4,4′-BBT derivatives by Stille coupling reaction with aryl halides (Method A in Scheme 1); in fact, the reaction gave **BBT-Ph^{t}Bu** in a moderate yield (44%).[11c] Likewise, the Stille coupling reaction of **BBT-Sn** with 4-bromobenzonitrile afforded **BBT-PhCN** with a 4-cyanophenyl group on each thiophene ring in a yield of 49%. Meanwhile, for Suzuki coupling reaction, we prepared **BBT-Br** by the dehydration of **SO-BBT-H4** using tetramethylethylenediamine (TMEDA) and then *n*-BuLi, followed by treatment with carbon tetrabromide (CBr_4). Thus, we conducted the Suzuki coupling reaction of **BBT-Br** with 4-*tert*-butylphenylboronic acid or 4-cyanophenylboronic acid at room temperature (25 °C) due to the thermal instability of **BBT-Br** (Method B in Scheme 1). As a result, **BBT-Ph^{t}Bu** and **BBT-PhCN** were successfully prepared by the Suzuki coupling reactions even at a low temperature, although the yields of the two BBT derivatives by Suzuki coupling reactions were lower than those by the Stille coupling reactions. Therefore, this result provides facile synthetic methods for the introduction of aryl substituents into the 1, 1′-positions on the thiophene rings of the 4,4′-BBT skeleton, that is, 1,1′-diaryl-4,4′-BBT derivatives by Stille and Suzuki coupling reactions.

A single-crystal X-ray structural analysis was successfully performed for **BBT-Ph^{t}Bu**, but unfortunately we could not obtain single crystals of **BBT-PhCN** with a sufficient size to make the X-ray structural analysis possible. (Fig. 2). The crystal structure of **BBT-Ph^{t}Bu** has two crystallographically independent molecules in which the dihedral angles between the two benzo[*c*]thiophene units are 127.61 and 126.90°, respectively (Fig. 2a). There are no short π–π contacts of less than 3.60 Å between the neighboring molecules (Fig. S3, ESI†), which indicates the absence of π–π stacking between the molecules. On the other hand, the formation of a one-dimensional continuous molecular chain by the intermolecular CH···S hydrogen bonding interactions[12] between the thiophene rings of neighboring molecules was observed in the crystal structure of **BBT-Ph^{t}Bu** (C(1)H(1)···S(3) angle = 162.85°, C(1)···S(3) distance = 3.833 Å, and H(1)···S(3) distance = 2.915 Å and C(55)H(55)···S(2) angle = 153.77°, C(55)···S(2) distance = 3.668 Å, and H(55)···S(2) distance = 2.792 Å, Fig. 2b). Meanwhile, the X-ray powder diffraction (XRD) patterns for **BBT-PhCN** as well as **BBT-Ph^{t}Bu** did not show diffraction peaks over 2θ = 20°, suggesting the absence of π–π stacking. On the other hand, the XRD patterns for **BBT-H** exhibited diffraction peaks at around 2θ = 22°, 26°, and 28°, suggesting the presence of π–π stacking (Fig. S4 in ESI†).

The photoabsorption and fluorescence spectra of **BBT-H**, **BBT-Ph^{t}Bu**, and **BBT-PhCN** in toluene are shown in Fig. 3a and their photophysical data are summarized in Table 1. **BBT-Ph^{t}Bu** and **BBT-PhCN** show intense photoabsorption bands (λ_{max}^{abs} = 386 nm and 399 nm, respectively) with relatively high molar extinction coefficients (ε_{max} = 20 700 M^{-1} cm^{-1} and 27 000 M^{-1} cm^{-1}, respectively) in longer wavelength regions by 27 nm and 40 nm, respectively, in comparison with **BBT-H** (λ_{max}^{abs} = 359 nm, ε_{max} = 7500 M^{-1} cm^{-1}), due to the expansion of the π-conjugated system by the introduction of an aryl substituent on the benzo[*c*]thiophene chromophore. The corresponding fluorescence bands (λ_{max}^{fl} = 469 nm and 472 nm) of **BBT-Ph^{t}Bu** and **BBT-PhCN** also appear in longer wavelength regions by 59 nm and 62 nm, respectively, in comparison with that (λ_{max}^{fl} = 410 nm) of **BBT-H**. Therefore, the Stokes shift (SS) values of **BBT-Ph^{t}Bu** and **BBT-PhCN** are 4585 cm^{-1} and 3876 cm^{-1}, respectively, which are larger than that (3465 cm^{-1}) of **BBT-H**. Meanwhile, the fluorescence quantum yield (Φ_{fl} = 0.27) of **BBT-PhCN** is lower than those (Φ_{fl} = 0.41 and 0.39, respectively) of **BBT-H** and **BBT-Ph^{t}Bu**. Time-resolved fluorescence spectroscopy demonstrated that the fluorescence lifetime (τ_{fl} = 1.27 ns) of **BBT-PhCN** is shorter than those (3.46 ns and 2.33 ns, respectively) of **BBT-H** and **BBT-Ph^{t}Bu**. The radiative rate constant (k_r = 2.13 × 10^8 s^{-1}) for **BBT-PhCN** is

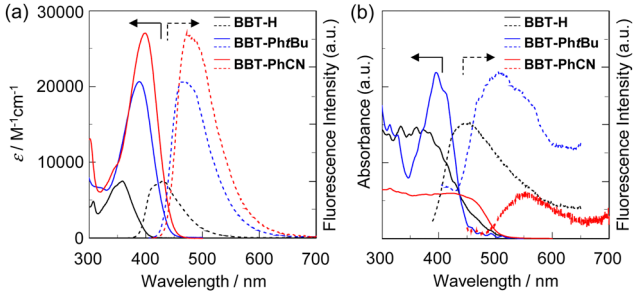

Fig. 3 (a) Photoabsorption (solid line) and fluorescence (dotted line) spectra of **BBT-H**, **BBT-Ph^{t}Bu** and **BBT-PhCN** (3.0×10^{-5} M) in toluene. (b) Solid-state UV-vis diffuse reflection–absorption (solid line) and fluorescence (dotted line) spectra (λ^{ex} = 360 nm for **BBT-H** and **BBT-Ph^{t}Bu** and 422 nm for **BBT-PhCN**) of the as-recrystallized **BBT-H**, **BBT-Ph^{t}Bu** and **BBT-PhCN**.

somewhat larger than those (1.18×10^8 s^{-1} and 1.63×10^8 s^{-1}, respectively) for **BBT-H** and **BBT-Ph^{t}Bu**, but the nonradiative rate constant ($k_{nr} = 5.75 \times 10^8$ s^{-1}) for **BBT-PhCN** is two to three times higher than those (2.62×10^8 s^{-1} and 1.70×10^8 s^{-1}, respectively) for **BBT-Ph^{t}Bu** and **BBT-H**. Consequently, the ratio of nonradiative constant to radiative constant (k_{nr}/k_r = 2.70) for **BBT-PhCN** is larger than those (1.44 and 1.56, respectively) for **BBT-H** and **BBT-Ph^{t}Bu**, indicating that the lower Φ_{fl} value of **BBT-PhCN** is mainly due to the larger k_{nr} value compared to those of **BBT-H** and **BBT-Ph^{t}Bu**. The larger k_{nr} value of **BBT-PhCN** may be induced by rotation between the electron-withdrawing cyanophenyl group and BBT fluorophore, leading to excited-state intramolecular charge transfer (ICT)-based fluorescence quenching.[13]

Moreover, the solid-state photophysical properties of **BBT-H**, **BBT-Ph^{t}Bu**, and **BBT-PhCN** have been investigated by using the solid-state UV-Vis diffuse reflection–photoabsorption and fluorescence spectral measurements (Fig. 3b) and their photophysical data are summarized in Table 2. **BBT-Ph^{t}Bu** in the solid state exhibits a photoabsorption maximum ($\lambda_{max}^{abs\text{-}solid}$) at 400 nm, which is similar to the photoabsorption spectrum in toluene (Fig. 3a). On the other hand, the photoabsorption bands of **BBT-H** and **BBT-PhCN** in the solid state are broadened in longer wavelength regions with an onset of *ca.* 500 nm, compared to those in toluene. In the corresponding solid-state fluorescence spectra, **BBT-H**, **BBT-Ph^{t}Bu**, and **BBT-PhCN** show fluorescence bands ($\lambda_{max}^{fl\text{-}solid}$ = 455 nm, 510 nm and 548 nm, respectively) in longer wavelength regions by 45 nm, 41 nm, and 76 nm, respectively, compared to those in toluene. The

Table 2 Photophysical data of 4,4′-bibenzo[*c*]thiophene derivatives in the solid state

Dye	$\lambda_{max}^{abs\text{-}solid}$/nm	$\lambda_{max}^{fl\text{-}solid}$/nm ($\Phi_{fl\text{-}solid}$)[a]
BBT-H	360[b]	455 (< 0.02)[b]
BBT-Ph^{t}Bu	400[b]	510 (0.04)[b]
BBT-PhCN	422	548 (< 0.02)

[a] Fluorescence quantum yields ($\Phi_{fl\text{-}solid}$) were determined by using a calibrated integrating sphere system (λ^{ex} = 360 nm for **BBT-H** and **BBT-Ph^{t}Bu** and 422 nm for **BBT-PhCN**). [b] Previous work (ref. 11*c*).

$\Phi_{fl\text{-}solid}$ values of **BBT-H**, **BBT-Ph^{t}Bu**, and **BBT-PhCN** in the solid state are <0.02, 0.04, and <0.02, respectively, which are significantly lower than those in toluene (Table 1). Thus, the precise evaluations of the $\tau_{fl\text{-}solid}$ values for the three derivatives were difficult due to their feeble solid-state fluorescence properties. In general, the bathochromic shifts of λ_{max}^{abs} and λ_{max}^{fl} and the lowering of the Φ_{fl} value by changing from the solution to the solid state is quite common and explained in terms of the formation of intermolecular π–π interactions or continuous intermolecular hydrogen bonding between the fluorophores in the solid state and consequent delocalization of excitons or excimers.[14] Thus, based on the XRD patterns for **BBT-H**, the bathochromic shift of λ_{max}^{fl} and the lowering of the Φ_{fl} value of **BBT-H** by changing from the solution to the solid state would be attributed to the formation of intermolecular π–π interactions between the molecules in the solid state. Meanwhile, based on the XRD patterns for **BBT-Ph^{t}Bu** and **BBT-PhCN** as well as the crystal structure of **BBT-Ph^{t}Bu**, the continuous intermolecular CH···S hydrogen bonding interactions between the neighboring molecules might be responsible for the aggregation-caused quenching (ACQ) of **BBT-Ph^{t}Bu** and **BBT-PhCN**.

The electrochemical properties of **BBT-H**, **BBT-Ph^{t}Bu**, and **BBT-PhCN** were investigated by cyclic voltammetry (CV) in acetonitrile or DMF containing 0.1 M tetrabutylammonium perchlorate (Bu_4NClO_4). The potentials were internally referenced to ferrocene/ferrocenium (Fc/Fc^+). The cyclic voltammograms of the three derivatives showed an irreversible oxidation at 0.88 V for **BBT-H**, 0.55 V for **BBT-Ph^{t}Bu**, and 0.73 V for **BBT-PhCN**, while any obvious reduction wave did not appear within the potential window (Fig. S5, ESI†). The oxidation waves for **BBT-Ph^{t}Bu** and **BBT-PhCN** were cathodically shifted by 0.33 V and 0.15 V, respectively, compared to that for **BBT-H**. This result indicates that the introduction of the electron-donating

Table 1 Photophysical and electrochemical data and the HOMO and LUMO energy levels of 4,4′-bibenzo[*c*]thiophene derivatives in solution

Dye	λ_{max}^{abs}/nm (ε_{max}/M^{-1} cm^{-1})[a]	λ_{max}^{fl}/nm (Φ_{fl})[b]	τ_{fl}/ns[c]	k_r/s^{-1}[d]	k_{nr}/s^{-1}[e]	k_{nr}/k_r	E_{onset}^{ox}/V[f]	E_g^{opt}/eV[g]	HOMO/eV[h]	LUMO/eV[h]
BBT-H	359 (7500)[i]	410 (0.41)[i]	3.46[i]	1.18×10^{8i}	1.70×10^{8i}	1.44[i]	0.75[i]	3.16[i]	−5.55[i]	−2.39[i]
BBT-Ph^{t}Bu	386 (20 700)[i]	469 (0.39)[i]	2.33[i]	1.68×10^{8i}	2.62×10^{8i}	1.56[i]	0.42[i]	2.87[i]	−5.22[i]	−2.35[i]
BBT-PhCN	399 (27 000)	472 (0.27)	1.27	2.13×10^8	5.75×10^8	2.70	0.59	2.82	−5.39	−2.57

[a] In toluene. [b] In toluene. Fluorescence quantum yields (Φ_{fl}) were determined by using a calibrated integrating sphere system (λ^{ex} = 359 nm, 386 nm and 399 nm for **BBT-H**, **BBT-Ph^{t}Bu**, and **BBT-PhCN**, respectively). [c] Fluorescence lifetime. [d] Radiative rate constant ($k_r = \Phi_{fl}/\tau_{fl}$). [e] Nonradiative rate constant ($k_{nr} = (1 - \Phi_{fl})/\tau_{fl}$). [f] Onset ($E_{onset}^{ox}$) *versus* Fc/Fc^+ of the oxidation potential. [g] Optical energy gaps (E_g^{opt}) were determined from the intersection (393 nm, 432 nm, and 439 nm for **BBT-H**, **BBT-Ph^{t}Bu**, and **BBT-PhCN**, respectively) of the photoabsorption and fluorescence spectra in toluene. [h] *Versus* vacuum level. [i] Previous work (ref. 11*c*).

tert-butylphenyl group and the electron-withdrawing cyanophenyl group into the benzo[*c*]thiophene skeleton causes the lowering of the oxidation potential. The HOMO energy levels ($-[E_{onset}^{ox} + 4.8]$ eV) *versus* vacuum level were estimated from the onset potentials (E_{onset}^{ox} = 0.75 V for **BBT-H**, 0.42 V for **BBT-Ph^{t}Bu**, and 0.59 V for **BBT-PhCN**) of the oxidation waves and the LUMO energy levels were estimated from the E_{onset}^{ox} and intersections (optical energy gap: E_g^{opt} = 3.16 eV for **BBT-H**, 2.87 eV for **BBT-Ph^{t}Bu**, and 2.82 eV for **BBT-PhCN**) of the photoabsorption and fluorescence spectra in toluene. The HOMO energy levels (−5.22 eV and −5.39 eV, respectively), of **BBT-Ph^{t}Bu** and **BBT-PhCN** are higher than that (−5.55 eV) of **BBT-H**. On the other hand, the LUMO energy levels (−2.39 eV and −2.35 eV, respectively) of **BBT-H** and **BBT-Ph^{t}Bu** are similar to each other, but the LUMO energy level (−2.57 eV) of **BBT-PhCN** is lower than that of **BBT-H**. Thus, this fact reveals that the bathochromic shift of the photoabsorption band from **BBT-H** to **BBT-Ph^{t}Bu** and **BBT-PhCN** is mainly attributed to the destabilization of the HOMO energy level for **BBT-Ph^{t}Bu** and the destabilization of the HOMO energy level and the stabilization of the LUMO energy level for **BBT-PhCN** through the introduction of the electron-donating *tert*-butylphenyl groups and the electron-withdrawing cyanophenyl groups, respectively, into the benzo[*c*]thiophene skeleton, leading to a decrease in the HOMO–LUMO band gap.

The electronic structures and molecular orbitals of **BBT-H**, **BBT-Ph^{t}Bu**, and **BBT-PhCN** were calculated by using DFT at the B3LYP/6-31G(d,p) level (Fig. S6, ESI†). The DFT calculations demonstrate that the HOMO for **BBT-H** is delocalized on each benzo[*c*]thiophene unit, but the HOMOs for **BBT-Ph^{t}Bu** and **BBT-PhCN** are delocalized on each benzo[*c*]thiophene unit and the aryl substituent. The LUMOs for **BBT-H** and **BBT-Ph^{t}Bu** are mainly delocalized over the whole benzo[*c*]thiophene skeleton through the 4,4′-positions, but the LUMO for **BBT-PhCN** is delocalized over the whole molecule containing cyanophenyl groups through the 4,4′-positions. It was found that the HOMO energy level (−5.06 eV) of **BBT-Ph^{t}Bu** is higher than that (−5.29 eV) of **BBT-H**, but the LUMO energy levels (−1.55 eV and −1.58 eV, respectively) of **BBT-H** and **BBT-Ph^{t}Bu** are similar to each other. The HOMO and LUMO energy levels (−5.64 eV and −2.32 eV, respectively) of **BBT-PhCN** are significantly lower than those of **BBT-H**, but the lowering in the LUMO energy level is larger than that in the HOMO energy level, although CV showed that the HOMO energy level of **BBT-PhCN** is higher than that of **BBT-H**. Nevertheless, the DFT calculations suggested that compared to **BBT-H**, the rise of the HOMO energy level for **BBT-Ph^{t}Bu** and the lowering of the LUMO energy level for **BBT-PhCN** result in a decrease in the HOMO–LUMO band gap (3.74 eV, 3.56 eV, and 3.32 eV, respectively), from **BBT-H** to **BBT-Ph^{t}Bu** and **BBT-PhCN**. Furthermore, time-dependent density functional theory (TD-DFT) calculations were performed to elucidate the photophysical properties of the three derivatives (Fig. S7, ESI†). The calculated $\lambda_{max}^{abs\text{-}calcd}$ and ε_{calcd} values of **BBT-H**, **BBT-Ph^{t}Bu**, and **BBT-PhCN** are 345 nm and 7800 M^{-1} cm^{-1}, 361 nm and 44300 M^{-1} cm^{-1}, and 403 nm and 38300 M^{-1} cm^{-1}, respectively. The $S_0 \rightarrow S_1$ transitions are mainly attributed to the transitions from the HOMO to the LUMO (67% for **BBT-H**, 88% for **BBT-Ph^{t}Bu**, and 93% for **BBT-PhCN**). Indeed, the TD-DFT calculations are in good agreement with the experimental results about bathochromic shifts of the photoabsorption bands from **BBT-H** to **BBT-Ph^{t}Bu** and **BBT-PhCN**, although the ε_{calcd} value of **BBT-PhCN** is lower than that of **BBT-Ph^{t}Bu**, which is opposite to the experimental results.

In conclusion, we developed facile synthetic methods of 1,1′-diaryl-4,4′-bibenzo[*c*]thiophene (-BBT) derivatives by Stille or Suzuki coupling reaction and their photophysical and electrochemical properties and X-ray crystal structures were elucidated sufficiently by an experimental approach and DFT calculations. Further studies on the synthetic routes from 1,1′-diaryl-4,4′-BBT derivatives to 1,1′,3,3′-tetraaryl-4,4′-BBT derivatives are now in progress to gain insight into the effect of aryl substituents on the photophysical and electrochemical properties of 4,4′-BBT derivatives.

Conflicts of interest

There are no conflicts to declare.

Acknowledgements

This work was supported by Grants-in-Aid for Scientific Research (B) from the Japan Society for the Promotion of Science (JSPS) KAKENHI Grant Number 22H02123.

Notes and references

1 (*a*) F. Wudl, M. Kobayashi and A. J. Heeger, *J. Org. Chem.*, 1984, **49**, 3382–3384; (*b*) O. D. Abrbanel, J. Rozon and G. R. Hutchison, *J. Phys. Chem. Lett.*, 2022, **13**, 2158–2164; (*c*) G. Grover, J. D. Tovar and M. Kertesz, *J. Phys. Chem. C*, 2022, **126**, 5302–5310.

2 Y.-C. Hu, Z.-L. Lin, T.-C. Huang, J.-W. Lee, W.-C. Wei, T.-Y. Ko, C.-Y. Lo, D.-G. Chen, P.-T. Chou, W.-Y. Hung and K.-T. Wong, *Mater. Chem. Front.*, 2020, **4**, 2029–2039.

3 J. D. Douglas, G. Griffini, T. W. Holcombe, E. P. Young, O. P. Lee, M. S. Chen and J. M. J. Fréchet, *Macromolecules*, 2012, **45**, 4069–4074.

4 Q. Liu, Q.-Y. Feng, H. Yamada, Z.-S. Wang, N. Ono, X.-Z. You and Z. Shen, *Chem. – Asian J.*, 2012, **7**, 1312–1319.

5 X. Chen, D. Zhang, Y. He, M. U. Ali, Y. Wu, C. Zhao, P. Wu, C. Yan, F. Wudl and H. Meng, *Mater. Chem. Front.*, 2020, **4**, 3578–3584.

6 (*a*) S. T. Meek, E. E. Nesterov and T. M. Swager, *Org. Lett.*, 2008, **10**, 2991–2993; (*b*) A. K. Mohanakrishnan and P. Amaladass, *Tetrahedron Lett.*, 2005, **46**, 4225–4229; (*c*) K. Kawabata and H. Goto, *J. Mater. Chem.*, 2012, **22**, 23514–23524; (*d*) U. Mitschke and P. Bäuerle, *J. Chem. Soc., Perkin Trans. 1*, 2001, 740–753; (*e*) J. W. Terpstra and A. M. van Leusen, *J. Org. Chem.*, 1986, **51**, 230–238; (*f*) R. M. El-Shishtawy, K. Fukunishi and S. Miki, *Tetrahedron Lett.*, 1995, **36**, 3177–3180.

7 (*a*) D.-T. Hsu and C.-H. Lin, *J. Org. Chem.*, 2009, **74**, 9180–9187; (*b*) A. Ishii, J. Nakayama, J. Kazami, Y. Ida, T. Nakamura and M. Hoshino, *J. Org. Chem.*, 1991, **56**, 78–82; (*c*) R. R. Amaresh, M. V. Lakshmikantham, J. W. Baldwin, M. P. Cava, R. M. Metzger and R. D. Rogers, *J. Org. Chem.*, 2002, **67**, 2453–2458.

8 E. Aqad, M. V. Lakshmikantham and M. P. Cava, *Org. Lett.*, 2004, **6**, 3039–3041.

9 Y. Shimizu, Z. Shen, S. Ito, H. Uno, J. Daub and N. Ono, *Tetrahedron Lett.*, 2002, **43**, 8485–8488.

10 P. Amaladass, J. A. Clement and A. K. Mohanakrishnan, *Eur. J. Org. Chem.*, 2008, 3798–3810.

11 (*a*) K. Obayashi, T. Higashino, K. Imato and Y. Ooyama, *New J. Chem.*, 2021, **45**, 13258–13261; (*b*) K. Obayashi, K. Imato, S. Aoyama, T. Enoki, S. Akiyama, M. Ishida, S. Suga, K. Mitsudo and Y. Ooyama, *RSC Adv.*, 2021, **11**, 18870–18880; (*c*) K. Obayashi, S. Miho, M. Yasui, K. Imato, S. Akiyama, M. Ishida and Y. Ooyama, *New J. Chem.*, 2021, **45**, 17085–17094.

12 (*a*) H. A. Fargher, T. J. Sherbow, M. M. Haley, D. W. Johnson and M. D. Pluth, *Chem. Soc. Rev.*, 2022, **51**, 1454–1469; (*b*) H. S. Karmakar, V. S. Kadam, A. L. Patel and S. S. Zade, *ChemistrySelect*, 2020, **5**, 5776–5780; (*c*) M. Domagała, S. J. Grabowski, K. Urbaniak and G. Mlostoń, *J. Phys. Chem. A*, 2003, **107**, 2730–2736.

13 (*a*) D. Liese and G. Haberhauer, *Isr. J. Chem.*, 2018, **58**, 813–826; (*b*) C. Yan, Z. Guo, W. Chi, W. Fu, S. A. A. Abedi, X. Liu, H. Tian and W.-H. Zhu, *Nat. Commun.*, 2021, **12**, 3869.

14 (*a*) H. Langhals, T. Potrawa, H. Nöth and G. Linti, *Angew. Chem., Int. Ed. Engl.*, 1989, **28**, 478–480; (*b*) H.-C. Yeh, W.-C. Wu, Y.-S. Wen, D.-C. Dai, J.-K. Wang and C.-T. Chen, *J. Org. Chem.*, 2004, **69**, 6455–6462; (*c*) Y. Ooyama, T. Nakamura and K. Yoshida, *New J. Chem.*, 2005, **29**, 447–456.